2018 IEEE Intelligent Vehicles Symposium (IV)
Changshu, Suzhou, China, June 26-30, 2018

Social Force Based Microscopic Modeling of Vehicle-Crowd Interaction

Dongfang Yang, Ümit Özgüner, *Life Fellow, IEEE*, and Keith Redmill

***Abstract*— Pedestrian safety is of paramount importance for intelligent transportation systems. This study focuses on the scenarios where pedestrians appear as crowds and interact with moving vehicles in a relatively-free space. Based on social force model (SFM), a vehicle-crowd interaction (VCI) model is proposed to describe both the behavior of crowd pedestrians and vehicle. Specifically, a heuristic-based and effective modeling of vehicle influence on pedestrians is designed and incorporated into the crowd-only SFM. Qualitative analysis of systematic simulations of various VCI scenarios demonstrates the effectiveness of the proposed model. This model can effectively describe the VCI scenarios such as vehicle approaching from different directions, vehicle zigzagging, and vehicle sharply turning.**

I. INTRODUCTION

Modeling and simulating the interactions between pedestrians and vehicles benefits the development of intelligent transportation systems (ITS) and autonomous vehicles (IV). This has always been a challenging problem. The challenges originate from the large varieties of pedestrian formations and the various possibilities of vehicle maneuvers. Pedestrians might appear to vehicles as individuals, smaller groups, or larger crowds, with different patterns depending on particular scenarios. Based on the spatial-temporal states of pedestrians, vehicles, either semi- or fully-autonomous, can generate various maneuvers, which will, in return, have different impact on pedestrian movement. The varieties of both the pedestrian movement and the vehicle maneuvers increase the difficulty of modeling and simulating this type of interaction.

This study focuses on the scenarios of crowd pedestrians interacting with vehicles in a relatively-free space. The word 'crowd' is defined as *a group of at least 5 individuals within the same space*, according to a similar definition in [1], but with some modifications. Here, the minimum number of pedestrians guarantees various interactive scenarios without reducing the problem into individual pedestrian cases, where the interaction among pedestrians is small, hence can be ignored. The relatively-free space refers to an wide enough area without specific lanes or marks in which pedestrians can freely move and the vehicle maneuvers can achieve the maximum steering angle (not usual in structured roads). Such area could be, for example, a shared space near a shopping center, an open parking lot, or a large corridor in the airport. Therefore, the problem is finding an effective approach to model and simulate the vehicle-crowd interaction (VCI), particularly for the crowds defined above and vehicles of relatively-free maneuvers.

All authors are with the Department of Electrical and Computer Engineering, The Ohio State University, Columbus, OH, 43210, USA {yang.3455, ozguner.1, redmill.1}@osu.edu

To build a valid VCI, first, we have to find a model that can effectively describe and simulate the crowd-only interaction, and then, the vehicle influence on pedestrians is incorporated into this model. There are many crowd-only interaction models that can generate close-to-reality crowd movements [1]. The social force model (SFM) was chosen due to its performance in terms of motion base cases, self-organization behavior, and model applicability [1]. SFM [2] describes the motion of each pedestrian as a combined effect of socially repulsive or attractive forces from the surrounding pedestrians, and a desire that drives the pedestrian to her destination. This model has been successfully utilized in different types of transportation related applications, for example, the crowd simulation of the loading and unloading at a bus station [3], the evaluation of the shared space design [4], and the simulation of the crowds crossing a signalized intersection [5].

This study benefits from two important characteristics of SFM: the exact position of each pedestrian at any time is accessible, and the interaction effect among pedestrians can be easily adjusted. These characteristics provide a setting that can comfortably incorporate the vehicle influence on pedestrians. Some studies have attempted to model this influence. In [5] for example, the vehicle influence is modeled as a monotonically decaying repulsive force perpendicular to the vehicle's contour, which is designed for a scenario where the crowd faces a turning vehicle at an intersection. Although this modeling generates satisfactory pedestrian behavior for the particular scenario, the lack of various vehicle maneuvers cannot guarantee the universality of the vehicle influence. In another study [4], the vehicle influence is modeled similar to the interaction effect among pedestrians in the crowd-only SFM but with increased magnitude and range. Various vehicle maneuvers are accomplished by mimicking the motion of the pedestrian but with constraints on the steering. This design still has two drawbacks. First, the pedestrian-similar modeling of vehicle influence fails to consider the shape of the vehicle and the interactive detail when the influence magnitude is large. Second, failing to use a proper vehicle model causes inaccurate vehicle maneuvers. To solve the above issues, our study introduced a new modeling of the vehicle influence that considers both the shape and longitudinal velocity of the vehicle. To accurately describe vehicle motion, the vehicle maneuvers obey the kinematic bicycle model [6] and are achieved by a lane-following controller [7] tracking the planned reference path. This configuration also provides convenience for the development of vehicle control algorithms in the future.

As the critical step before real-world implementation, sim-

978-1-5386-4452-2/18/$31.00 ©2018 IEEE

ulation plays an important role for the evaluation of the VCI model. In our previous study [8], a simulation platform that specifies several fundamental VCI scenarios facilitated the evaluation by providing straightforward animations and the easy accessibility of every states. In this study, the simulation is further optimized in terms of the scenario selection, the model parameter tuning, the qualitative analysis, and the computational efficiency.

The remainder of the paper is organized as follows. First, section 2 outlines the framework of the VCI model. Second, section 3 describes the incorporation of the vehicle influence on pedestrians into this model. Next, section 4 explains the kinematic bicycle model and the lane following controller. Followed by that, the simulation design and the model evaluation process are presented in section 5. Then, section 6 demonstrates the simulation result of various VCI scenarios. Last, conclusions and future work can be found in section 7.

II. FRAMEWORK

Building on the social force model (SFM) [2], the motion of each pedestrian is governed by 2-D Newtonian dynamics, assuming plane surface. The overall influence that causes the motion of a pedestrian i at time t can be described as a resultant force $F_i(t) \in \mathbb{R}^2$ consisting of sub-forces:

$$F_i(t) = \sum_{j \in \mathbb{Q}(i)} (f_r^{ij}(t) + f_c^{ij}(t) + f_n^{ij}(t)) + \beta_i(f_v^i(t)) \cdot f_d^i(t) + f_v^i(t) + f_b^i(t) + \epsilon_i(t). \quad (1)$$

In the above expression, $\mathbb{Q}(i)$ denotes the index set of the nearby pedestrians of the subject pedestrian i, and $f_r^{ij}(t), f_c^{ij}(t), f_n^{ij}(t)$ denote the repulsive (attractive) force, the collision force, and the navigational force from pedestrian j to pedestrian i, respectively. Together these forces are referred as social forces. $f_v^i(t)$ represents the vehicle influence on pedestrian i, which is also a repulsive force with a specific direction. $f_d^i(t)$ is the destination force that drives the pedestrian to the current destination. $\beta_i(f_v^i(t)) \in [0, 1]$ adjusts the magnitude of $f_d^i(t)$. The last two terms $f_b^i(t)$ and $\epsilon_i(t)$ denote forces from the physical boundaries and the random noise, respectively, which are reserved for future use. Using the resultant force, the dynamics equation is

$$\frac{d^2 x_i(t)}{dt^2} = \frac{v_i(t)}{dt} = a_i(t) = \frac{F_i(t)}{m}. \quad (2)$$

In the following text, the time index (t) will be omitted for convenience.

A. The Social Forces

The social forces $f_r^{ij}, f_c^{ij}, f_n^{ij}$ can be expressed in three aspects: magnitude, anisotropy and direction, as follows:

$$f_r^{ij} = -h(|d_{ij}|, d_r^0, f_r^m, \sigma_r) \cdot \mathbb{A}_r(\phi_{ij}, \lambda_r) \cdot \vec{e}_{ij} \quad (3)$$
$$f_c^{ij} = -h(|d_{ij}|, d_c^0, f_c^m, \sigma_c) \cdot \vec{e}_{ij} \quad (4)$$
$$f_n^{ij} = h(|d_{ij}|, d_n^0, f_n^m, \sigma_n) \cdot \mathbb{A}_n(\phi_n, \lambda_n) \cdot \vec{e}_n. \quad (5)$$

The magnitudes of the above forces all share a monotonically decaying relationship $h(.)$ with respect to the distance

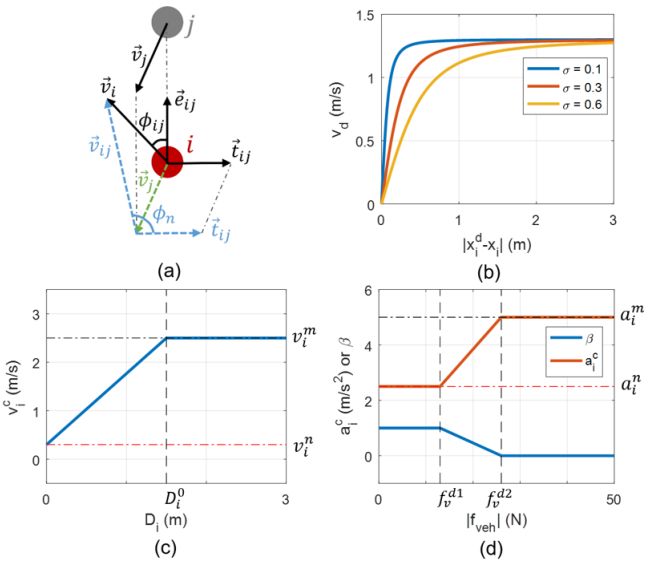

Fig. 1. (a) Illustration of notations in repulsive and navigational forces; (b) The effect of different σ_d; (c) The constraint on the velocity; (d) The constraint on the acceleration and the adjustment factor β_i

from pedestrian j to pedestrian i. A specific smooth decaying function is used to describe this relationship [9]:

$$h(d, d_0, M, \sigma) = \frac{M}{2d_0} \cdot \left(d_0 - d + \sqrt{(d_0 - d)^2 + \sigma}\right) \quad (6)$$

where d is the distance variable, M is the magnitude at zero distance, d_0 is a threshold where the magnitude reaches zero, and σ is the parameter that smooths the force around d_0.

Anisotropy $\mathbb{A}(.)$ is a property that modifies the magnitude when pedestrian j is approaching from different angles. f_c^{ij} does not have anisotropy because physical touch happens equally in all directions. f_r^{ij} and f_n^{ij} have different anisotropies defined below, respectively:

$$\mathbb{A}_r(\phi_{ij}, \lambda_r) = \lambda_r + (1 - \lambda_r) \cdot \frac{1 + \cos(\phi_{ij})}{2} \quad (7)$$
$$\mathbb{A}_n(\phi_n, \lambda_n) = \exp(-\lambda_n \cdot \phi_n) \quad (8)$$
$$\forall \phi_{ij} < |\phi_{ij}^0| \quad , \quad \forall \phi_n < |\phi_n^0| \quad (9)$$

where λ_r, λ_n modifies the anisotropy characteristics, $\phi_{ij} = \angle(\vec{v}_i, \vec{e}_{ij})$, $\phi_n = \angle(\vec{v}_{ij}, \vec{t}_{ij})$, as illustrated in figure 1 (a), and $|\phi_{ij}^0|$, $|\phi_n^0|$ define the effective field of view.

The direction $\vec{e}_{ij}$ is the unit vector from pedestrian i to pedestrian j, and $\vec{e}_n = \text{sign}(\vec{v}_{ij} \cdot \vec{t}_{ij}) \cdot \vec{t}_{ij}$, where $\vec{t}_{ij}$ is a unit vector perpendicular to $\vec{e}_{ij}$, as illustrated in figure 1(a).

B. Destination Force

The destination force functions like a proportional controller, as shown below:

$$f_d^i = k_d \cdot (v_i - v_i^d) \quad (10)$$

where k_d is the control gain that regulates the current velocity v_i to match the desired velocity v_i^d, which is defined as:

$$v_i^d = |v_i^0| \cdot \frac{x_i^d - x_i}{\sqrt{|x_i^d - x_i|^2 + \sigma_d^2}}. \quad (11)$$

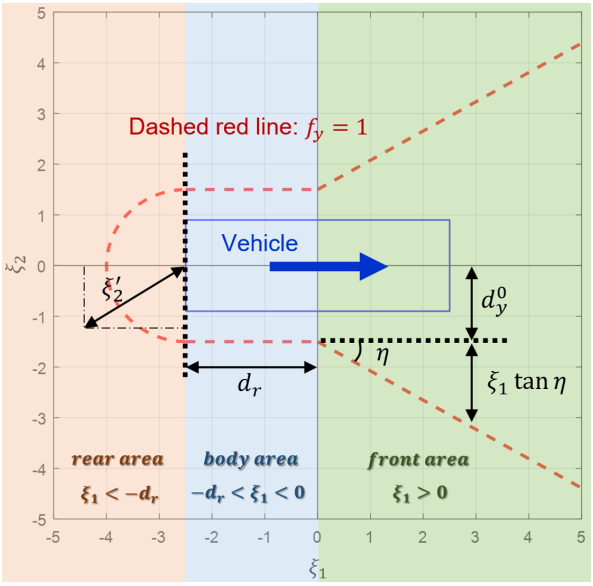

Fig. 2. Illustration of the vehicle influence modeling

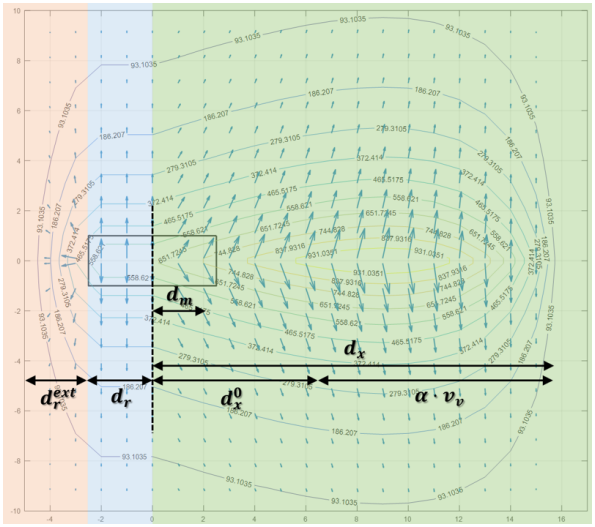

Fig. 3. The magnitude (contours and arrow lengths) and direction (arrow directions) of vehicle influence with the modeling parameters

Here, $|v_i^0|$ is the mean preferred walking speed according to statistic data. x_i^d is the current destination. σ_d is a parameter that reduces the velocity when the pedestrian is getting close to the destination [9], as illustrated in figure 1(b).

C. Constraints and Adjustment

Constraints on both the velocity v_i and the acceleration a_i of a pedestrian i are dependent on the density of nearby pedestrians D_i and the vehicle influence f_v^i:

$$|v_i| \leq v_i^c(D_i), \ |a_i| \leq a_i^c(f_v^i) \tag{12}$$

D_i is measured as the distance from the subject pedestrian to the closest pedestrian in front. Smaller D_i means higher pedestrian density. As shown in figure 1(c), different values of D_i result in different constraints on the velocity v_i:

$$v_i^c = \begin{cases} v_i^n + \frac{D_i}{D_i^0} \cdot (v_i^m - v_i^n) & , D_i < D_i^0 \\ v_i^m & , D_i > D_i^0. \end{cases} \tag{13}$$

When the vehicle influence is large, the pedestrian will try to quickly leave the dangerous area and therefore reduce the desire to go to the destination. This characteristics is modeled as the change of a_i^c and β_i, as shown in figure 1(d):

$$a_i^c = \begin{cases} a_i^n & , |f_v^i| < f_v^{d1} \\ a_i^n + \frac{|f_v^i| - f_v^{d1}}{f_v^{d2} - f_v^{d1}} \cdot (a_i^m - a_i^n) & , f_v^{d1} < |f_v^i| < f_v^{d2} \\ a_i^m & , |f_v^i| > f_v^{d2} \end{cases} \tag{14}$$

$$\beta_i = \begin{cases} 1 & , |f_v^i| < f_v^{d1} \\ 1 - \frac{|f_v^i| - f_v^{d1}}{f_v^{d2} - f_v^{d1}} & , f_v^{d1} < |f_v^i| < f_v^{d2} \\ 0 & , |f_v^i| > f_v^{d2} \end{cases} \tag{15}$$

where f_v^{d1} and f_v^{d2} are two thresholds determined by the vehicle influences at distances that characterize danger.

III. VEHICLE INFLUENCE

Considering the local coordinates with the origin at the center of vehicle and assuming that the vehicle is heading to the positive x-axis. The vehicle influence can be described as the multiplication of longitudinal effect f_x, lateral effect f_y, and direction $\vec{n}$:

$$f_v^i = f_x \cdot f_y \cdot \vec{n}. \tag{16}$$

Let $\xi = (\xi_1, \xi_2)^T$ be the position of a pedestrian in the local coordinates. Depending on ξ, f_v^i differs in 3 areas: the front area ($\xi_1 > 0$), the body area ($-d_r < \xi_1 < 0$), and the rear area ($\xi_1 < -d_r$), as shown in figure 2.

A. Front Area

In the front area, an outward angle η defines the major influence region, which is enclosed by the red dashed line in figure 2. Both f_x and f_y are modeled as follows:

$$f_x = \frac{1}{2d_x}\left(-(\xi_1 - d_x) + \sqrt{(\xi_1 - d_x)^2}\right) \tag{17}$$

$$f_y = A_y \cdot \exp\left(-b_y(|\xi_2| - d_y)\right) \tag{18}$$

$$d_x = d_x^0 + \alpha \cdot |v_v| \tag{19}$$

$$d_y = d_y^0 + \xi_1 \tan\eta \tag{20}$$

$$\vec{n} = \begin{bmatrix} \cos(\text{sign}(\xi_2) \cdot \zeta(\xi_1)) \\ \sin(\text{sign}(\xi_2) \cdot \zeta(\xi_1)) \end{bmatrix} \tag{21}$$

$$\zeta = \begin{cases} \frac{\pi}{2} - \Delta\zeta_m \cdot \frac{d_x - d_m - \xi_1}{d_x - d_m} & , \forall \xi_1 > d_m \\ \frac{\pi}{2} - \Delta\zeta_m \cdot \xi_1 & , \forall \xi_1 < d_m. \end{cases} \tag{22}$$

d_x is the look-ahead distance where the longitudinal effect vanishes, which is a function of the vehicle velocity $|v_v|$ with parameters d_x^0 and α, as shown in figure 3. f_y decreases along the lateral direction. d_y is the distance where the lateral effect is constant ($f_y = A_y$). ζ is a small angle that changes the force direction $\vec{n}$, which is dependent on ξ_1 with parameters $\Delta\zeta_m$ and d_m. The change of force directions can be visualized in figure 3.

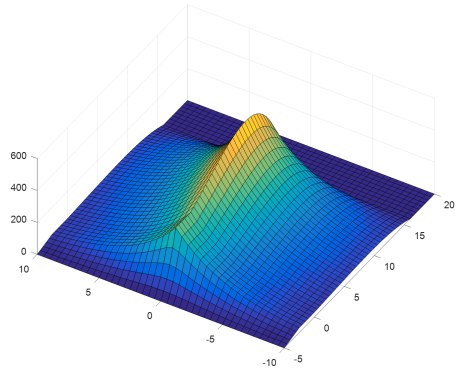

Fig. 4. The surface plot of the vehicle influence magnitude

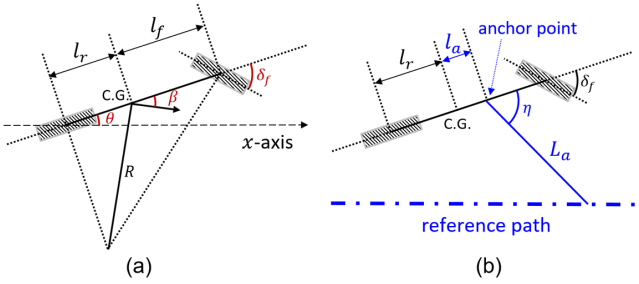

Fig. 5. (a) Kinematic bicycle model; (b) Lane-following controller.

B. Body Area

In the body area, $f_x = 1$ doesn't change. f_y decreases as the lateral distance increases. $\vec{n}$ points to the lateral direction.

$$f_x = 1 \tag{23}$$
$$f_y = A_y \cdot \exp\left(-b_y(|\xi_2| - d_y^0)\right) \tag{24}$$
$$\vec{n} = \begin{bmatrix} \cos(\text{sign}(\xi_2) \cdot \frac{\pi}{2}) \\ \sin(\text{sign}(\xi_2) \cdot \frac{\pi}{2}). \end{bmatrix} \tag{25}$$

C. Rear Area

In the rear area, f_x is defined similarly in the front area, with d_x being the vanishing point. f_y now decreases as the distance from the rear-center to the pedestrian position increases. $\vec{n}$ points from the rear-center to the pedestrian.

$$f_x = \frac{1}{2d_r^{ext}}\left(\xi_1 + d_x + \sqrt{(\xi_1 + d_x)^2}\right) \tag{26}$$
$$f_y = A_y \cdot \exp\left(-b_y(|\xi_2'| - d_y^0)\right) \tag{27}$$
$$d_x = d_r + d_r^{ext} \tag{28}$$
$$\xi_2' = \sqrt{(\xi_1 + d_r)^2 + \xi_2^2} \tag{29}$$
$$\vec{n} = \begin{bmatrix} \cos(\xi_1 + d_r) \\ \sin(\xi_2). \end{bmatrix} \tag{30}$$

The resulting vehicle influence direction and magnitude are illustrated in figure 3 and figure 4, respectively.

IV. Vehicle Maneuvers

The kinematic bicycle model [6] is used for generating vehicle maneuvers. This model has three assumptions: (a) the vehicle has planner motion; (b) both left and right wheels steer the same angle; and (c) there is no slip at both front and rear tires. It is applicable when the vehicle moves at relatively low speed, which is the case for most scenarios in this study. As illustrated in figure 5(a), let $x_v \in \mathbb{R}^2$ and $\theta_v \in \mathbb{R}$ be the position and the orientation of the vehicle, the model can be described as:

$$\dot{x}_v^1 = v_v \cos(\theta_v + \beta_v) \tag{31}$$
$$\dot{x}_v^2 = v_v \sin(\theta_v + \beta_v) \tag{32}$$
$$\dot{v}_v = f(u) \tag{33}$$
$$\dot{\theta}_v = \frac{v_v}{l_r} \sin\beta_v \tag{34}$$
$$\beta_v = \arctan\left(\frac{l_r}{l_f + l_r}\tan\delta_f\right) \tag{35}$$

where v_v is the longitudinal speed, β_v is the velocity angle with respect to the vehicle center of gravity (C.G.), l_f, l_r are the distances from C.G. to the front wheel and the rear wheel, respectively, u is the longitudinal control action (brake/gas), and δ_f is the lateral control action (steering angle of the front wheel). The longitudinal speed v_v is regulated by a P-controller. To follow the reference path specified in different interaction scenarios, the steering is achieved by a lane-following controller [7]:

$$\delta_f = -\tan^{-1}\left(\frac{(l_f + l_r)\sin\eta_v}{\frac{L_a}{2} + l_a\cos\eta_v}\right). \tag{36}$$

With this configuration, different realistic vehicle maneuvers can be generated so that various interaction scenarios can be designed and evaluated.

V. Simulation and Evaluation

A. Simulation

The simulation is done in Matlab. Since the VCI model is continuous, the Smart Euler method is applied to discretize the motion of pedestrian in Newtonian dynamics (2):

$$\begin{cases} v_i(t + \Delta t) = v_i(t) + a_i(t) \cdot \Delta t \\ x_i(t + \Delta t) = x_i(t) + \frac{1}{2}\left(v_i(t) + v_i(t + \Delta t)\right) \cdot \Delta t. \end{cases} \tag{37}$$

Different scenarios are designed by specifying the starting points and the destinations for pedestrians and providing the reference path and the desired velocity for the vehicle.

The effectiveness of the VCI model depends on the correct choices of model parameters, which are shown in table I. In this study, an effective parameter set is determined by visual inspection and qualitative analysis of individual pedestrian behavior in the simulation.

As an example of the computational efficiency, in a scenario of 20 pedestrians and 1 vehicle, an average running time of $0.11s$ for one step is achieved on windows 10 platform with Intel Core i5-4590 @ 3.30GHz CPU and 8GB memory. Although this does not reach real-time simulation (in the study $\Delta t = 0.05s$), with this performance, the computational efficiency can be further improved and finally lead to real-time simulation by making the simulation program more concise and by shifting the simulation platform from Matlab to a more efficient one, e.g., C++ based platforms.

TABLE I

AN EFFECTIVE PARAMETER SET TUNED BY VISUAL INSPECTION AND QUALITATIVE ANALYSIS

Type	Notation	Values
Repulsion	$\psi_r = (d_r^0, f_r^m, \sigma_r, \lambda_r, \phi_{ij}^0)$	$(2, 130, 0.4, 0.8, 300)$
Collision	$\psi_c = (d_c^0, f_c^m, \sigma_c)$	$(0.3, 500, 0.9)$
Navigation	$\psi_n = (d_n^0, f_n^m, \sigma_n, \lambda_n, \phi_n^0)$	$(7, 300, 0.4, 3, 240)$
Destination	$\psi_d = (k_d, \lvert v_i^0 \rvert, \sigma_d)$	$(230, unif(1.1, 1.5), 0.09)$
Vehicle	$\psi_v = (A_y, b_y, d_x^0, d_y^0, \alpha, \eta, d_m, \Delta\zeta_m, d_r, d_r^{ext})$	$(450, 0.25, 12, 1.5, 1, \pi/6, 1, \pi/6, 2.5, 2.5)$
Constraints	$\psi_l = (v_i^n, v_i^m, D_i^0, a_i^n, a_i^m)$	$(0.3, 2.5, 1.5, 2.5, 5)$

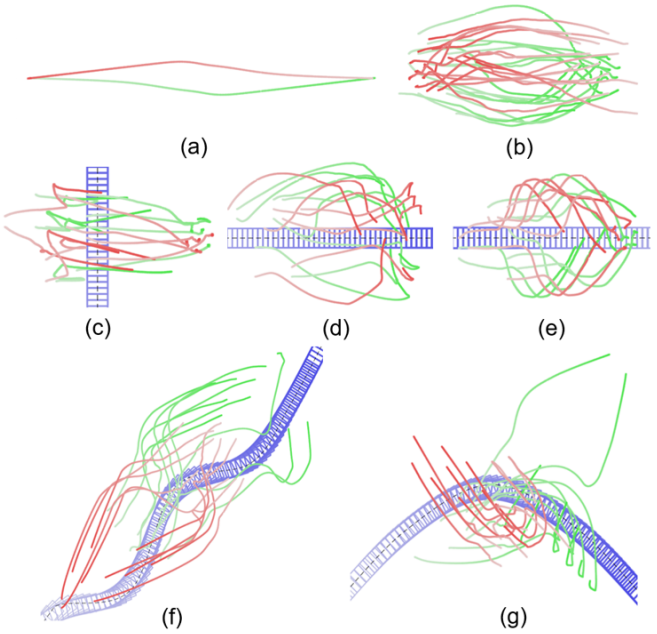

Fig. 6. Simulation trajectories: (a) one-on-one; (b) two crowds; (c)(d)(e) basic VCI scenarios; (f) vehicle zigzagging; (g) vehicle sharply turning.

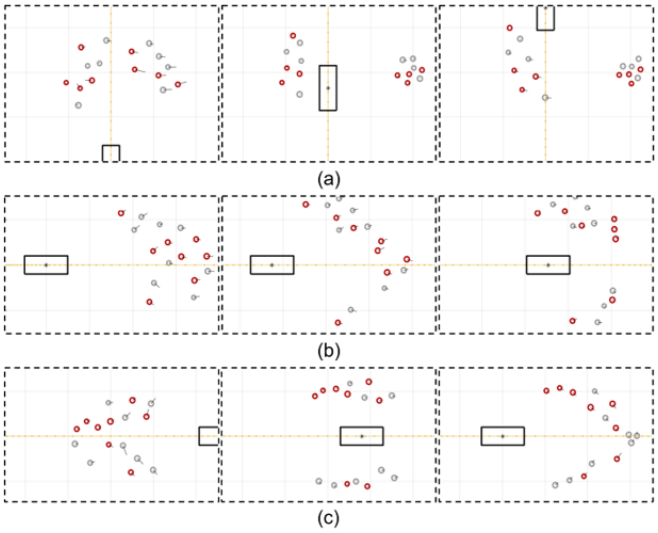

Fig. 7. Animation snapshots of basic scenarios: (a) lateral interaction; (a) back interaction; (c) front interaction.

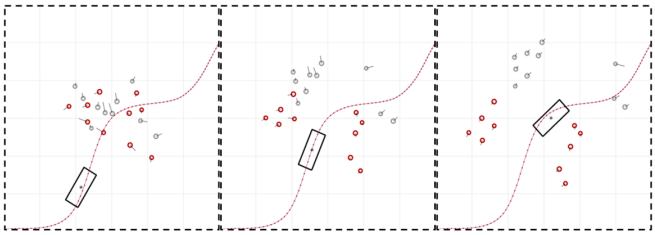

Fig. 8. Animation snapshots of vehicle zigzagging through the crowd.

B. Scenarios Design

The VCI model are evaluated by 3 classes of scenarios. They are designed from the basic ones to relatively complex ones, which are sufficient to test the model effectiveness.

- Pedestrian-only scenarios: pedestrian one-on-one, and two crowds encountering.
- Basic VCI scenarios: lateral interaction, back interaction, and front interaction.
- Complex VCI scenarios: vehicle zigzagging through the crowd and vehicle sharply turning into the crowd.

VI. RESULT

Figure 6 shows the simulation trajectories of both the vehicle and pedestrians. The red and green lines indicate pedestrian trajectories, with different colors dividing them into two groups. The blue rectangles indicate the vehicle trajectory. For all trajectories, the darker the color, the later the simulation time. In basic VCI scenarios, as shown in figure 6(c)(d)(e), there is no difference for the two pedestrian groups, while in other scenarios, each group have different starting points and destinations. From trajectory result, pedestrian behaviors such as avoiding, waiting, and detouring can be identified, which are sufficient to demonstrate the model effectiveness for the pedestrian-only scenarios.

For the VCI scenarios, a more detailed evaluation is required. Figure 7 displays the animation snapshots of all the basic VCI scenarios. Figure 8 and 9 present the snapshots of the complex VCI scenarios. The microscopic behavior of each pedestrian can be evaluated qualitatively in this way.

As an example of qualitative evaluation, we analyzed the microscopic behavior of a particular pedestrian in the last scenario, as indicated in blue color in figure 9. Figure 10 shows the record of a_i, a_i^c, v_i, v_i^c, $|f_v|$, $|f_d|$, and $\beta_i \cdot |f_v|$ of this pedestrian. At $t = 4s$, the density of nearby pedestrians D_i is high, hence v_i^c is reduced. At $t = 10s$, the pedestrian is experiencing high vehicle influence $|f_v|$, hence a_i^c is increased and $|f_d|$ is reduced due to β_i. All the changes match the spatial-temporal relationship in figure 9. Furthermore, as

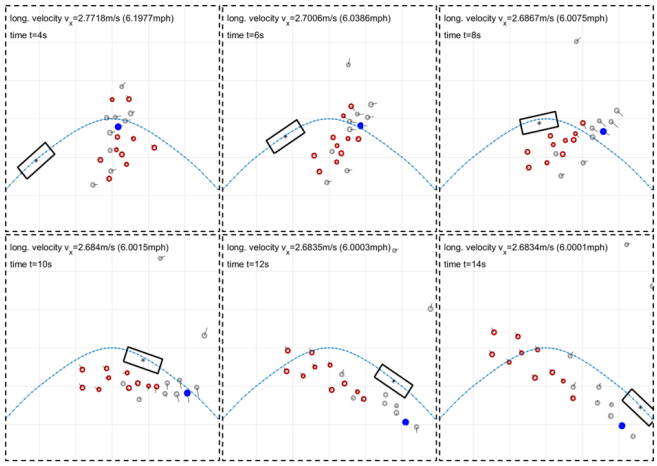

Fig. 9. Animation snapshots of vehicle sharply turning into the crowd.

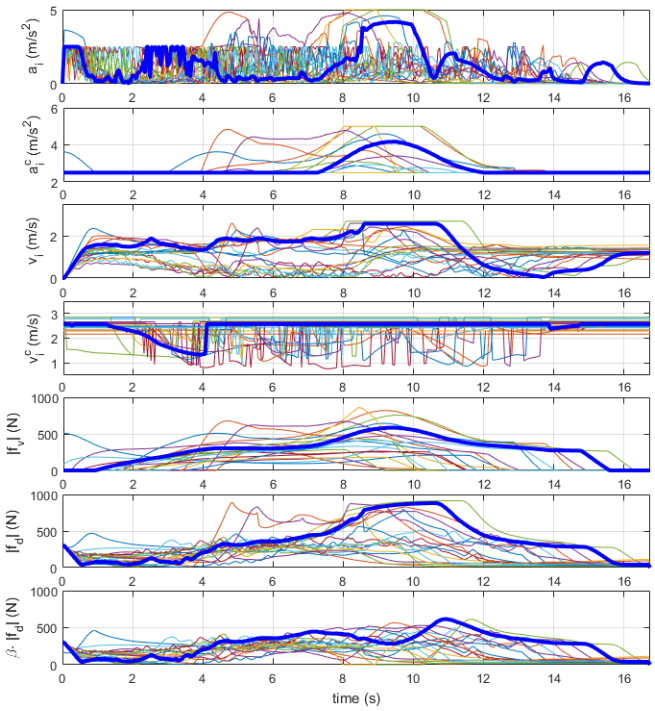

Fig. 10. Numerical results of the vehicle sharply turning scenario, with the bold blue line indicating the data of the reference pedestrian, and other colors representing other pedestrians.

shown in figure 11, the non-negative closest distances among all pedestrians indicates no violation of physical laws.

Similar qualitative analysis was applied to other scenarios. All the animated simulations can be accessed in the associated video submission[1].

VII. CONCLUSIONS

In conclusion, this study proposed a social force based vehicle-crowd interaction (VCI) model that can effectively describe various VCI scenarios. The qualitative analysis of the simulation result demonstrated the model effectiveness.

[1]https://youtu.be/Nh9w1VkF10U

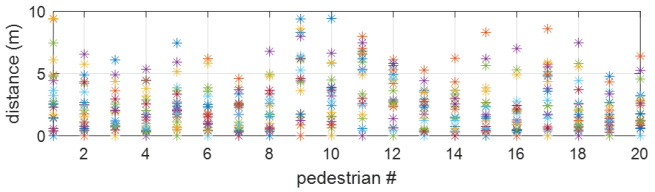

Fig. 11. The closest distances among all pedestrians in last scenario.

This model is beneficial to various ITS and IV applications such as pedestrian tracking in complex interaction situations and vehicle motion planning in the crowds.

Potential improvement lies in two aspects. One is to utilize realistic VCI data to further calibrate the model that has only been calibrated by visual inspection and qualitative analysis. Data-based calibration can apply approaches such as maximum likelihood estimation (MLE) and genetic algorithm (GA). The other improvement originates from the model itself. Some aspects of modeling might not perfectly describe the nature of the interaction, while other aspects might be redundant. In terms of real-world implementation, it also requires the development of vehicle control algorithms for specific scenarios and the reliability of pedestrian detection systems.

ACKNOWLEDGMENT

Material reported here was partially supported by the NSF under the CPS Program (Award 1528489 and 1446735) and partially by the United States Department of Transportation under Award Number 69A3551747111 for the Mobility21 University Transportation Center.

Any opinions, findings, conclusions, or recommendations expressed herein are those of the authors and do not necessarily reflect the views of the United States Department of Transportation or Carnegie Mellon University.

REFERENCES

[1] D. C. Duives, W. Daamen, and S. P. Hoogendoorn, "State-of-the-art crowd motion simulation models," *Transportation research part C: emerging technologies*, vol. 37, pp. 193–209, 2013.

[2] D. Helbing and P. Molnar, "Social force model for pedestrian dynamics," *Physical review E*, vol. 51, no. 5, p. 4282, 1995.

[3] E. Adamey, A. Kurt, and U. Ozguner, "Agent-based passenger modeling for intelligent public transportation," in *International IEEE Conference on Intelligent Transportation Systems*, pp. 255–260, 2013.

[4] B. Anvari, M. G. Bell, A. Sivakumar, and W. Y. Ochieng, "Modelling shared space users via rule-based social force model," *Transportation Research Part C: Emerging Technologies*, vol. 51, pp. 83–103, 2015.

[5] W. Zeng, P. Chen, G. Yu, and Y. Wang, "Specification and calibration of a microscopic model for pedestrian dynamic simulation at signalized intersections: A hybrid approach," *Transportation Research Part C: Emerging Technologies*, vol. 80, pp. 37–70, 2017.

[6] Ü. Özgüner, T. Acarman, and K. A. Redmill, *Autonomous ground vehicles*. Artech House, 2011.

[7] Y. Kuwata, J. Teo, S. Karaman, G. Fiore, E. Frazzoli, and J. P. How, "Motion planning in complex environments using closed-loop prediction," in *Proc. AIAA Guidance, Navigation, and Control Conf. and Exhibit*, 2008.

[8] D. Yang, A. Kurt, K. Redmill, and Ü. Özgüner, "Agent-based microscopic pedestrian interaction with intelligent vehicles in shared space," in *Proceedings of the 2nd International Workshop on Science of Smart City Operations and Platforms Engineering*, pp. 69–74, ACM, 2017.

[9] R. El Helou, "Agent-based modelling of pedestrian microscopic interactions," Master's thesis, The Ohio State University, 2016.